The plasma-membrane Ca^{2+}-ATPase of *Leishmania donovani* is an extrusion pump for Ca^{2+}

Debjani MANDAL*, Tanmoy MUKHERJEE*, Sibaji SARKAR†, Sabita MAJUMDAR‡ and Amar BHADURI*§

*Leishmania Group, Enzyme Division and ‡Biophysics Division, Indian Institute of Chemical Biology, 4 Raja S.C. Mullick Road, Calcutta-700 032, India and †241 Lineberger Comprehensive Cancer Center CB no. 7295, University of North Carolina, Chapel Hill, NC 27599, U.S.A.

Controlled exposure of *Leishmania donovani* promastigotes to hypotonic shock results in the formation of deflagellated unsealed ghosts of original polarity that largely retain the pellicular microtubular structure associated with plasma membrane of the parasite. Gentle shearing followed by suspension of the purified membrane in appropriate isotonic buffer containing Mg^{2+} (4 mM) results in the formation of sealed everted vesicles. The presence of Mg^{2+} (4 mM) appears to be essential for efficient sealing and also to prevent leakiness. ATP-dependent Ca^{2+} accumulation can be demonstrated in these vesicles. K_m values for Ca^{2+} and ATP were 125 nM and 0.8 mM respectively. The accumulated Ca^{2+} reaches a concentration of 1.1 mM. Ca^{2+} uptake is completely inhibited by vanadate (40 μM) and several thiol-modifying agents. Using 5,5′-dithiobis-(2-nitrobenzoic acid) as the modifying agent, an excellent correlation between loss of enzyme activity and transport capability and their parallel regeneration in the presence of 2 mM dithiothreitol was demonstrated. Using 2′,7-bis(carboxyethyl)-5(6)-carboxyfluorescein as the fluorescent pH probe, it was observed that Ca^{2+} entry into the vesicles is accompanied by an outward movement of H^+ from the vesicles. Taken together, this paper establishes that the high-affinity transmembrane Ca^{2+}-ATPase [Ghosh, Ray, Sarkar and Bhaduri (1990) J. Biol. Chem. **265**, 11345–11351; Majumdar, Mukherjee, Ray and Bhaduri (1992) J. Biol. Chem. **267**, 18440–18446] is an extrusion pump for Ca^{2+} in this human pathogen.

INTRODUCTION

The messenger role of Ca^{2+} is now firmly established in many higher eukaryotes and in some lower eukaryotes including such free-living protozoa as *Paramecium* spp. [1–3]. The control of numerous diverse cellular functions is attained by regulation of the free cytoplasmic concentration of Ca^{2+}. In general, controlled movement of Ca^{2+} across plasma and organelle membranes leads to a transitory rise in cytoplasmic free Ca^{2+} concentration. This, in turn, allows interaction of increased cytoplasmic Ca^{2+} with target proteins and enzymes which initiates a cascade of biochemical reactions. The transitory rise is followed by rapid removal of excess cytoplasmic Ca^{2+}, which re-establishes Ca^{2+} homeostasis in the cytoplasm [4]. There are a few well-defined mechanisms for removal of excess cytoplasmic Ca^{2+} against a steep concentration gradient. Energy-dependent extrusion of Ca^{2+} from its site of action has been established as a major mechanism of Ca^{2+} removal in several cellular systems. A decade of intense work from several laboratories has clearly established that in sarcoplasmic reticulum and red blood cells, transmembrane high-affinity Ca^{2+}-ATPases act as true extrusion pumps for Ca^{2+}, although the detailed molecular mechanisms for such processes remain to be elucidated [5–8]. The presence of well-characterized high-affinity Ca^{2+}-ATPases with demonstrated capability of translocating Ca^{2+} across the membrane is thus strongly indicative of a biomodulatory role for Ca^{2+} in the functioning of a particular cell type or in the physiology of an organism.

Leishmania donovani is an important member of the kinetoplastida group of parasites. The human pathogen is the causative agent for visceral leishmaniasis or Kala-azar, a fatal disease that is endemic in many parts of the tropical world [9]. The organism has a digenic life cycle. The flagellated promastigote or vector form enters liver macrophages and quickly undergoes morphogenetic transformation to the aflagellated amastigote form in the phagolysosomal complex of the macrophages [10]. This cellular differentiation which leads to pathogenicity is most probably dependent on some as yet unidentified signal from the macrophage milieu. The biochemical nature of the signal, its transduction processing and amplification remain to be elucidated. Although no convincing evidence has so far been produced to implicate Ca^{2+} directly in the process, an elaborate mechanism for Ca^{2+} metabolism appears to exist in the promastigote, the cultured form of the organism and other related kinetoplastida. With the use of permeabilized cells, the presence of two internal pools of Ca^{2+} other than the cytoplasmic pool have been demonstrated in various trypanosomes, including *Leishmania* spp. [11–15]. We have recently shown that sudden exposure to an increase in environmental temperature, as is encountered by *L. donovani* promastigotes in the host, results in a rapid rise in cytoplasmic free Ca^{2+} concentration, which is primarily due to its release from the internal non-mitochondrial pool [16]. We have previously demonstrated the presence of a high-affinity Ca^{2+}-ATPase in the plasma membrane of *L. donovani* promastigotes that apparently needs no exogenous Mg^{2+} for catalytic activity. The enzyme spans the plasma membrane, with its catalytic site oriented towards the cytoplasm [17,18], suggesting that it is an extrusion pump for Ca^{2+}. In this report we describe a method for producing sealed plasma-membrane vesicles of *L. donovani* promastigotes of defined polarity. Using these everted vesicles we have demonstrated the ability of the Ca^{2+}-ATPase to act as an extrusion pump for Ca^{2+}. Moreover, the movement of Ca^{2+} is accompanied by a counter movement of H^+, the stoichiometry of which could

Abbreviations used: DCCD, *N,N*-dicyclohexylcarbodi-imide; CCCP, carbonyl cyanide *m*-chlorophenylhydrazone; FCCP, carbonyl cyanide *p*-(trifluoromethyoxy)phenylhydrazone; DTNB, 5,5′-dithiobis-(2-nitrobenzoic acid); pCMB, *p*-chloromercuribenzoic acid; MMTS, methyl methane thiosulphonate; DTT, dithiothreitol; BCECF, 2′,7-bis(carboxyethyl)-5(6)-carboxyfluorescein; calcein, 2′,7′-{[bis (carboxymethyl) amino]methyl}-fluorescein; p[NH]ppA, adenosine 5′-[β,γ-imido]triphosphate.

§ To whom correspondence should be addressed.

not be established because of the presence of a powerful H^+-translocating Mg^{2+}-ATPase of the same orientation in the plasma membrane. A preliminary report of this work has been presented [19].

MATERIALS AND METHODS

Chemicals and radiochemicals

All biochemicals were purchased from Sigma, unless otherwise mentioned. 2′,7-Bis(carboxyethyl)-5(6)-carboxyfluorescein (BCECF) was from Molecular Probes. [γ-^{32}P]ATP (approx. 3000 Ci/mmol) was from Bhaba Atomic Research Centre, and $^{45}Ca^{2+}$ (5–50 mCi/mg) was from Amersham.

Organism

The organism used in this work is a clinical isolate from a patient with confirmed Kala-azar and the strain is designated MHOM/IN/1978/UR-6. The cells were grown and maintained in a solid blood/agar medium that has been described elsewhere [20].

Enzyme assay

Glucose-6-phosphate dehydrogenase, hexokinase, isocitrate dehydrogenase and malate dehydrogenase were measured by conventional spectrophotometric methods. Asparate transcarbamylase was assayed colorimetrically as described by Mukherjee et al. [21]. Succinate dehydrogenase was measured by phenazine methosulphate-mediated reduction of 2,6-dichlorophenol-indophenol [22]. Plasma-membrane 3′-nucleotidase and Mg^{2+}-ATPase were assayed by the method of Ghosh et al. [17] and Majumdar et al. [18] respectively.

Ca^{2+}-ATPase was assayed both colorimetrically and with [γ^{32}-P]ATP. The details of these assay procedures have also been described by Ghosh et al. [17]. Unless otherwise stated, EGTA (200 μM) was used as the chelating agent for Ca^{2+}, and free cytoplasmic Ca^{2+} concentration was calculated as described by Sillen and Martell [23].

Measurement of $^{45}Ca^{2+}$ transport

For transport experiments, an appropriate amount of vesicles (about 100 μg of protein) was suspended in 0.5 ml of 25 mM Hepes/Tris buffer, pH 7.4, containing 125 mM KCl, 15 mM NaCl, 4 mM $MgCl_2$ and 200 μM EGTA. After preincubation for 10 min at 28 °C, various concentrations of $^{45}Ca^{2+}$ (2.5 μCi) were added to provide the desired final free Ca^{2+} concentration. The transport reaction was initiated by the addition of ATP (3 mM) after 10 min of preincubation. Appropriate control tubes were run in parallel without ATP. Filtration was carried out at the desired time intervals with a nitrocelluose membrane (0.45 μm porosity) and rapidly washed with 5 ml of suspension buffer containing EGTA (2 mM). Filters were removed to vials containing 10 ml of scintillation fluid for counting.

Protein measurement

Protein was determined by a modified Lowry method for membrane proteins containing SDS in the reagent [24].

Electron microscopy

Samples were fixed with 3 % glutaraldehyde for 14–16 h at 4 °C. After a wash with the respective buffers, the samples were post-fixed with 1 % osmium tetroxide in Kellenburger buffer for 16–20 h at room temperature. The pellets were then washed again and dehydrated with a graded series of ethanol solutions and finally embedded in SPURRT resin. Thin sections were collected using an ultrathin microtome and picked up on copper grids. Observations were made in a transmission electron microscope (JEOL IN ex) at different magnifications.

Preparation of sealed vesicles

L. donovani promastigotes of 72 h growth on solid medium [20] were collected and washed twice with buffer A (25 mM Tris/HCl, pH 7.4, 50 mM KCl and 5 mM $MgCl_2$). Wet washed cells (2 g) were suspended in 100 ml of 5 mM Tris/HCl buffer pH 7.4, with 0.5 mM PMSF in four long glass tubes in ice. The tubes were vortex-mixed in a cyclomixer seven to eight times for a total period of 60 min with 10 min intervals between each mixing. The cell suspension was centrifuged at 3300 ***g*** in a Sorvall SS-34 rotor for 20 min at 4 °C. The supernatant at this stage was stored for marker enzyme measurement. The pellet was washed once with the same buffer and finally suspended in 20 ml of buffer A and designated the unsealed ghost (see Figure 1, top). To prepare sheared membranes, this ghost suspension was then homogenized in a Potter/Elvehjem homogenizer and centrifuged at 13200 ***g*** for 15 min. The pellet was once again suspended in 30 ml of buffer A and again homogenized as above and finally diluted to a total volume of 90 ml with buffer B (buffer A containing 1.6 M sucrose). A 22.5 ml aliquot of this suspension was then gently layered over 7.5 ml of buffer B and centrifuged in a Sorvall AH-629 rotor at 49000 ***g*** for 36 min at 4 °C. The layer formed above the 1.6 M sucrose was collected by transfer with a Pasteur pipette. This was designated the sheared plasma membrane. For final sealing this fraction was mixed with an equal volume of buffer C (25 mM Hepes/Tris, pH 7.4, 125 mM KCl, 15 mM NaCl and 4 mM $MgCl_2$). After gentle mixing with buffer C, membrane was collected by centrifugation at 13200 ***g*** and gently resuspended in 10 ml of buffer C. It was then allowed to stand for 60 min at 4 °C with gentle shaking. Sealed vesicle formation took place at this stage. Sealed vesicles were finally centrifuged at 17000 ***g*** and resuspended in an appropriate volume of buffer C (see Figure 1, bottom) and used for subsequent experiments. The average internal volume of the vesicles was determined by the retention of labelled RbCl and inulin. The vesicles were loaded with either ^{86}RbCl or [^{14}C]Inulin during the sealing process and then filtered, washed and counted as described by Rottenberg [25]. The calculated average internal volume of vesicles was 1.4 μl/mg of protein.

Monitoring of the internal pH of sealed vesicles

BCECF at a concentration of 4 μg/ml was mixed with buffer C. Vesicles were sealed as described above. Subsequently the vesicles were washed twice with ice-cold buffer C to remove excess extracellular dye and finally suspended in buffer C. For fluorescence measurements, the dye-loaded vesicles of final density about 500 μg of protein/ml were placed in a 1 ml fluorescence cuvette. An Hitachi spectrofluorimeter model F4010 was used to monitor the readings of BCECF at 505 nm excitation and 525 nm emission wavelengths [26]. No appreciable leakage of the dye was observed during the period in which the experiments were completed.

RESULTS

Characterization of vesicle preparation

Pioneering cytological studies established that flagellated trypanosomatids contain a structurally unique cytoskeletal microtubular arrangement that is closely associated with the inner lamina of the plasma membrane of intact cells [27]. This

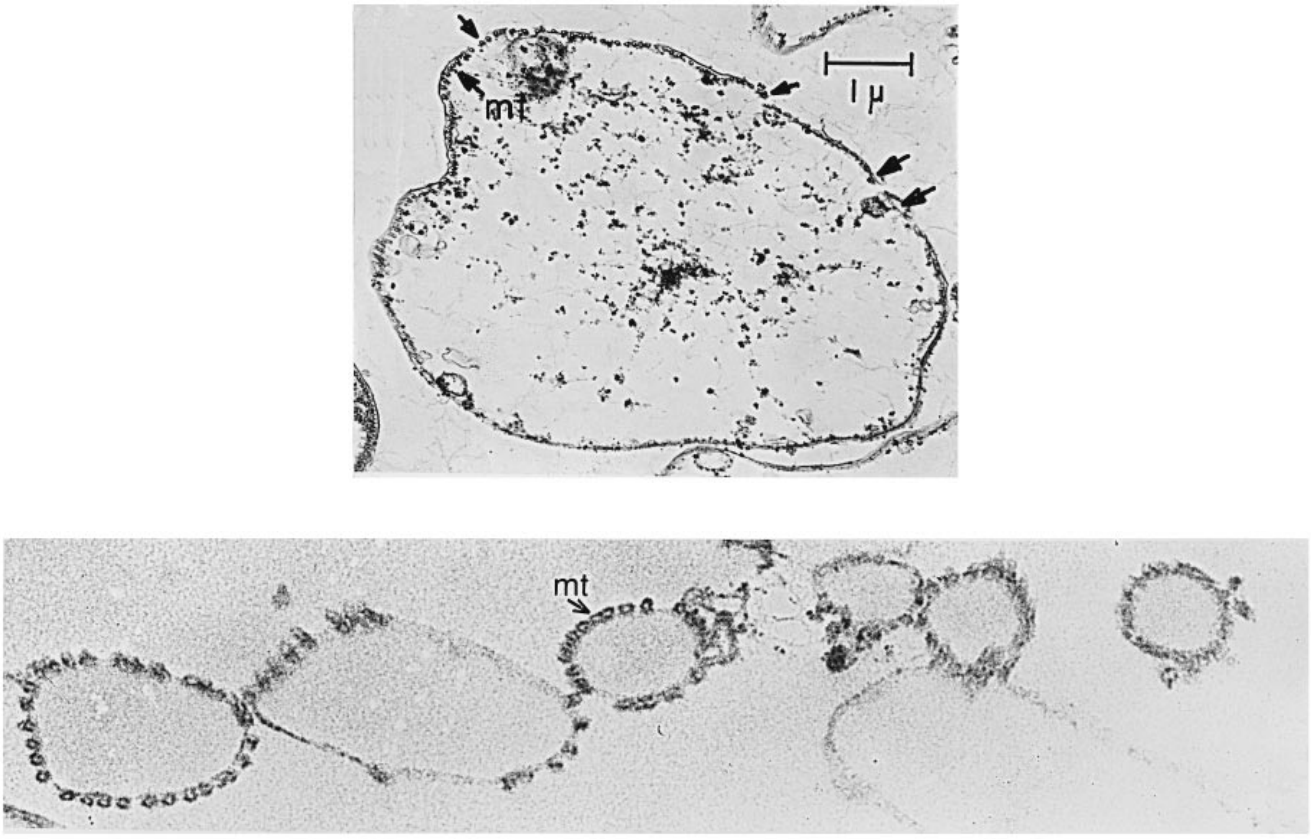

Figure 1 Thin section electron micrograph of a single crude ghost (top; × 12000) and everted plasma-membrane vesicles (bottom; × 45000)

mt, microtubules; arrows indicate discontinuity in plasma membrane.

arrangement apparently provides scaffolding for the membrane structure and can be used to determine polarity of membrane vesicles. Dwyer [28] showed that isolated membranes of *L. donovani*, obtained after disruption of cells, partially retained the original microtubule structure. On the basis of this observation, a comparatively gentle procedure involving controlled hypotonic shock but excluding drastic homogenization was developed for preparing deflagellated round unsealed ghosts of original polarity (Figure 1, top). Cytoplasmic marker enzymes, e.g. glucose-6-phosphate dehydrogenase and isocitrate dehydrogenase, along with hexokinase, a marker enzyme for glycosome, a unique organelle of kinetoplastida [27], were all completely (> 95 %) released into the medium. In contrast, both the 3′-nucleotidase, the classic marker ectozyme for all *Leishmania* spp. [29], and Ca^{2+}-ATPase, the catalytic site of which was now accessible to added ATP [18], were exclusively present (> 95 %) in the unsealed ghost (results not shown). This unsealed ghost preparation was previously used by us to characterize the regulatory properties of Ca^{2+}-ATPase in its membrane-bound form [18].

Thin section study under the electron microscope revealed that vesicles obtained from the sheared membranes of the unsealed ghosts mostly retained their microtubular structure and were largely everted, as indicated by marker microtubules. These vesicles had diameters between 1.5 and 3.0 μm. Further, the vesicles did not show any obvious discontinuity and appeared to be sealed (Figure 1, bottom). Sealing of vesicles was confirmed with the help of the fluorescent dye calcein by exploiting its self-quenching property at high concentrations [30] and also by Rb^+ trapping [25]. Total scanning of the field revealed the presence of some broken membranes and a few vesicles of original polarity (results not shown). Assuming that the ectoenzyme 3′-nucleotidase is completely inaccessible in completely sealed everted vesicles, only 50–65 % of its total activity ($n = 5$) was inaccessible. Presumably, apart from broken membranes and vesicles of original polarity, a fraction of the everted vesicles remained unsealed.

In order to evaluate the sealing potential at various stages of everted vesicle preparation and also to ascertain the role of various ions in facilitating the sealing process, a set of experiments were conducted; the results are summarized in Table 1. The accumulated results show that, if the correct osmomolarity is maintained with either sucrose (250 mM) or salts, everted membrane vesicle formation from sheared membranes occurs quite efficiently in the presence of Mg^{2+} ion (4 mM) alone. The requirement for Mg^{2+} appears to be essential as univalent cations such as Na^+ or K^+ even at high concentrations were completely ineffective and Mn^{2+} could barely help in sealing. In contrast, we were unable to demonstrate even partial sealing of unsealed ghosts under any of these conditions by employing the Ca^{2+}-translocation assay or calcein (see above) as the fluorescent probe. Interestingly, when employing the calcein assay, we observed that, for sealing of sheared membranes, Mg^{2+} could be completely replaced by Ca^{2+} (5 mM) in sucrose (250 mM) as the suspending medium. For obvious technical reasons, the ATP-dependent $^{45}Ca^{2+}$-uptake assay could not be used in this case (results not shown). We also observed that everted vesicles

Table 1 ATP-dependent Ca^{2+} accumulation under various conditions of sealing

For each sealing experiment, the appropriate ghost or membrane preparation (1 mg of protein) was suspended in a total volume of 4 ml containing 25 mM Tris/Hepes buffer, pH 7.4, and other ingredients as indicated below and given under Sealing conditions. The incubation mixture was allowed to shake gently for 30 min at 4 °C. At the end of the sealing period, the temperature was raised to 28 °C and a suitable amount was transferred from each individual tube to 0.6 ml of assay medium at 28 °C containing 25 mM Tris/Hepes buffer, pH 7.4, 200 μM $CaCl_2$ (2.5 μCi), 200 μM EGTA and all other ingredients originally used for sealing at their respective sealing concentrations. For example, for tube no. 5, the incubation medium for the Ca^{2+}-uptake assay contained sucrose (250 mM) and Mg^{2+} (5 mM) along with the reagents stated above. The reaction was immediately initiated by the addition of 3 mM ATP. Ca^{2+} accumulation was allowed to proceed for 10 min. Subsequent washing and counting were as described in the Materials and methods section. For each tube, a control without ATP was run in parallel and the data presented are after subtraction of this value.

Tube no.	Stages of vesicle preparation	Sealing conditions	Ca^{2+} uptake (nmol/mg of protein)
1	Unsealed ghost		0.009
2	Unsealed ghost	Sucrose (250 mM), Mg^{2+} (10 mM)	0.010
3	Unsealed ghost	KCl (125 mM), NaCl (15 mM), Mg^{2+} (10 mM)	0.010
4	Sheared membrane	Sucrose (250 mM)	0.030
5	Sheared membrane	Sucrose (250 mM), Mg^{2+} (5 mM)	0.800
6	Sheared membrane	Sucrose (250 mM), Mg^{2+} (10 mM)	0.930
7	Sheared membrane	NaCl (140 mM)	0.020
8	Sheared membrane	KCl (140 mM)	0.025
9	Sheared membrane	KCl (130 mM), Mn^{2+} (10 mM)	0.095
10	Sheared membrane	KCl (125 mM), NaCl (15 mM)	0.026
11	Sheared membrane	KCl (125 mM), NaCl (15 mM), Mg^{2+} (2 mM)	1.0
12	Sheared membrane	KCl (125 mM), NaCl (15 mM), Mg^{2+} (4 mM)	1.60
13	Sheared membrane	KCl (125 mM), NaCl (15 mM), Mg^{2+} (10 mM)	1.66

largely failed to retain trapped $^{86}Rb^{+}$ when the vesicles were washed free of Mg^{2+} by repeated centrifugation in the absence of Mg^{2+} (results not shown). Mg^{2+} is apparently needed not only for sealing but also to prevent leakiness.

Ca^{2+} entry and accumulation in everted vesicles

Figure 2 demonstrates that the entry and accumulation of Ca^{2+} is totally dependent on the presence of exogenous ATP. At a concentration of 1.7 μM Ca^{2+}, $^{45}Ca^{2+}$ uptake at the end of 10 min was about 1.6 nmol/mg of membrane protein. On the basis of an average internal vesicle volume of 1.4 μl per mg of protein (see the Materials and methods section), the concentration of accumulated Ca^{2+} at steady-state was calculated to be 1.1 mM. The addition of the Ca^{2+} ionophore A23187 (10 μM) resulted in a rapid release of accumulated Ca^{2+}. The addition of 100 mM NaCl at the end of 10 min of Ca^{2+} uptake failed to release any accumulated Ca^{2+}, ruling out the presence of a Na^{+}/Ca^{2+} anitporter in the plasma membrane of the parasite (results not shown). For this experiment, Ca^{2+} uptake was measured in the original transport medium (see the Materials and methods section) from which NaCl was completely omitted and replaced by additional KCl.

Kinetic characterization of Ca^{2+} entry

The Ca^{2+}-ATPase appears to be a high-affinity pump for Ca^{2+}. When the concentration of free Ca^{2+} was varied over a wide range with EGTA as the chelator, and ATP (3 mM) was kept well above the saturating concentration, strictly hyperbolic kinetics were obtained (Figure 3). The half-maximal velocity for Ca^{2+} entry was calculated to be at 125 nM free Ca^{2+}. At saturating concentrations of free Ca^{2+}, the K_m for ATP was determined to be 0.8 mM (results not shown).

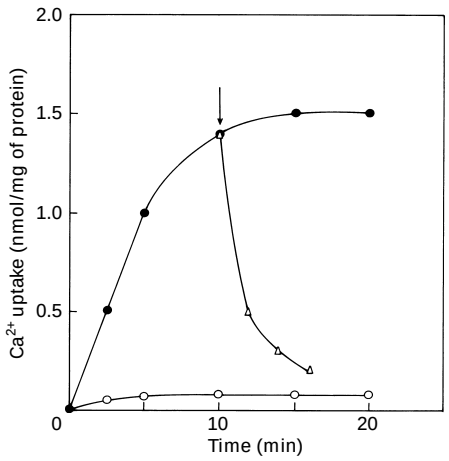

Figure 2 $^{45}Ca^{2+}$ uptake by everted vesicles

The composition of each assay tube was 25 mM Tris/Hepes buffer, pH 7.4, 125 mM KCl, 15 mM NaCl, 5 mM $MgCl_2$, 200 μM EGTA and 200 μM $CaCl_2$ (2.5 μCi) in a total volume of 0.5 ml. After preincubation for 10 min at 28 °C, the reaction was initiated by the addition of ATP (3 mM). Reactions were terminated at the indicated times. The arrow indicates addition of A23187 (10 μM) in a parallel experiment. ○, without ATP; ●, with ATP; △, after addition of A23187.

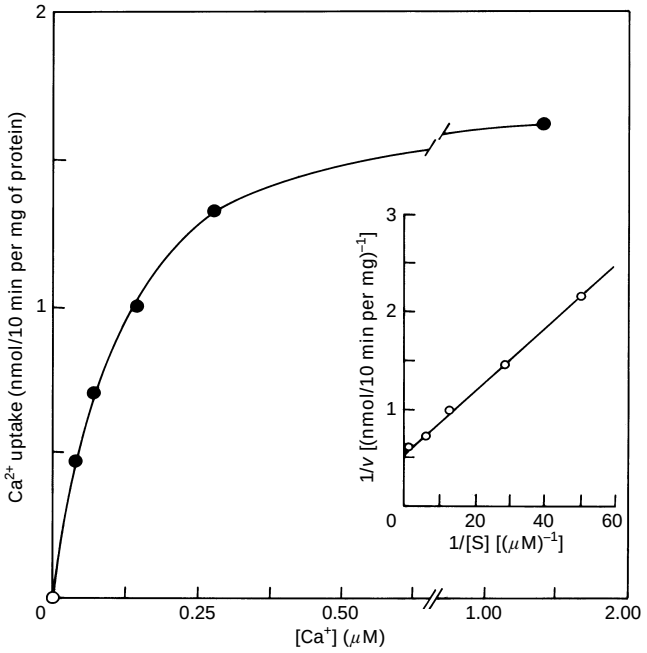

Figure 3 Kinetics of Ca^{2+} accumulation with varying Ca^{2+} concentration

The assay medium was the same as in Figure 2 except that the concentration of free Ca^{2+} was controlled by the addition of various concentrations of $CaCl_2$ to each tube. The incubation time for all tubes was 10 min. The rest of the assay procedure was the same as in Figure 2. The inset shows a Lineweaver–Burk plot of the same data.

Table 2 Nucleotide specificity of Ca^{2+} transport

Transport of $^{45}Ca^{2+}$ was measured under conditions described in Figure 2. Reactions were started with the 2 mM concentration of different nucleotides at a fixed Ca^{2+} concentration of 1.7 μM. n.d., not detected. Values in parentheses are percentages.

Addition	$^{45}Ca^{2+}$ accumulation (nmol/10 min per mg)	
ATP	1.60	(100)
p[NH]ppA	n.d.	(< 0)
UTP	0.04	(< 3.0)
CTP	0.04	(< 3.0)
GTP	0.07	(< 5.0)
PEP	0.01	(< 1.0)
ADP	0.01	(< 1.0)
ADP	0.01	(< 1.0)

Table 3 Effect of various inhibitors and modifiers on $^{45}Ca^{2+}$ uptake

For this experiment the vesicles were preincubated for 10 min with the indicated concentration of inhibitor or modifier. Reaction was started with 2 mM ATP, and $^{45}Ca^{2+}$ accumulation was observed from 10 min at a Ca^{2+} concentration of 1.7 μM. CCCP, carbonyl cyanide *m*-chlorophenylhydrazone; pCMB, *p*-chloromercuribenzoate; DTNB, dithiobis-(2-nitrobenzoic acid); MMTS, methyl methane thiosulphonate.

Inhibitor/modifier	$^{45}Ca^{2+}$ uptake (nmol/mg)	Inhibition (%)
None	1.50	–
Oligomycin (2 μg/ml)	1.41	7.0
Ouabain (2 mM)	1.42	6.0
DCCD (20 μg)	1.35	10.0
CCCP (5 μM)	1.44	4.0
Orthovanadate (40 μM)	0.04	97.0
pCMB (500 μM)	0.04	97.0
DTNB (500 μM)	0.03	98.0
MMTS (500 μM)	0.06	96.0

Nucleotide specificity for Ca^{2+} transport

Table 2 shows that Ca^{2+} uptake is exclusively dependent on ATP and no other nucleotide phosphate or phosphoenolpyruvate could replace it to any significant extent. As expected, adenosine 5′-[β,γ-imidotriphosphate (p[NH]ppA), the non-hydrolysable analogue of ATP, failed to drive any Ca^{2+} transport. We were unable to establish stoichiometry between ATP hydrolysis and Ca^{2+} transport because of the presence of a powerful Mg^{2+}-ATPase with the same orientation as that of Ca^{2+}-ATPase in the plasma membrane of the parasite [31]. The Mg^{2+}-ATPase was simultaneously activated during Ca^{2+}-transport studies because of the obligatory presence of Mg^{2+} (4 mM) in the medium. Conventional inhibitors of Mg^{2+}-ATPase, e.g. *N*,*N*-dicyclohexylcarbodi-imide (DCCD), failed to inhibit the activity of this enzyme completely even at very high concentrations.

Effect of inhibitors and modifiers on Ca^{2+} transport

Table 3 summarizes the results of inhibition studies in the presence of some inhibitors and potential modifiers. Low concentrations of vanadate completely blocked the transport and accumulation of $^{45}Ca^{2+}$, suggesting this enzyme to be a conventional P-type ion-motive ATPase [2]. The protonophore CCCP had no effect on transport. DTNB, pCMB and MMTS, all chemical modifiers of thiol groups on protein surfaces, blocked the transport completely at fairly low concentrations. Clearly

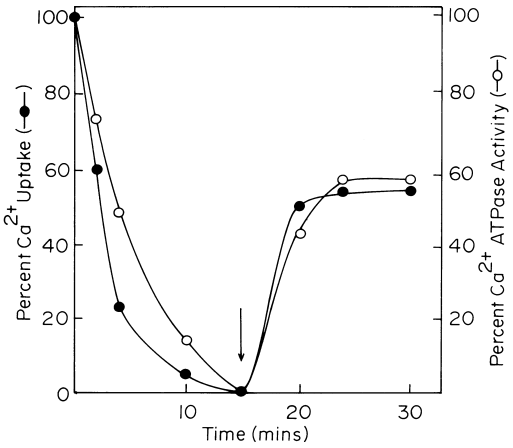

Figure 4 Correspondence between Ca^{2+}-ATPase activity and $^{45}Ca^{2+}$ uptake

The composition of each tube for this experiment was the same as in Figure 2 except that in all tubes except for the zero-time control, DTNB (500 μM) was added. For reversal of activity and transport property, DTT (2 mM; ↓) was added to a few tubes as indicated. Activity was measured as $[^{32}P]P_i$ release (see Materials and methods section) by removing suitable aliquots. Transport activity was measured as described.

Ca^{2+} translocation is dependent on one or more functional thiols in the enzyme.

Correlation between Ca^{2+}-ATPase activity and Ca^{2+} translocation

ATP-dependent Ca^{2+} entry into the vesicle appears to be exclusively mediated by the Ca^{2+}-ATPase. This became evident when an excellent correlation between activity of the enzyme and transport of Ca^{2+} could be demonstrated in the presence of 0.5 mM DTNB. When the everted vesicles were preincubated with DTNB for various lengths of time, the transport property and the Ca^{2+}-ATPase activity were lost in parallel (Figure 4). The addition of DTT (2 mM) at this stage rapidly restored nearly 60 % of both the activity and the transport property.

Ca^{2+} entry is accompanied by H^+ extrusion

The $Ca^{2+}+$ATPase of red blood cells has been thoroughly analysed as an extrusion pump for Ca^{2+}. Recently, using a liposomal system in which purified Ca^{2+}-ATPase was incorporated in the lipid bilayer, Hao et al. [8] convincingly showed that Ca^{2+} entry is an electrogenic process and the Ca^{2+}/H^+ stoichiometry for the entry process is 1:1. Owing to the presence of the powerful Mg^{2+}-ATPase on the surface of the sealed vesicle we were unable to quantitatively analyse the relationship between Ca^{2+} entry and H^+ extrusion. However, by using BCECF, a fluorophore that senses changes in pH, we obtained strong indications that entry of Ca^{2+} into the vesicle is accompanied by movement of H^+ in the opposite direction. Figure 5(A) is the control that demonstrates Mg^{2+}-ATPase to be a H^+-translocating pump. Activation of the enzyme results in rapid acidification of the vesicle. The proton gradient collapses on addition of FCCP. Addition of Ca^{2+} after the proton gradient has been established results in a comparatively small but definite alkalinization of the medium (Figure 5B). Obviously the functional Mg^{2+}-ATPase has prevented the complete collapse of the gradient. Alternatively, when Ca^{2+} and ATP were added simultaneously, the apparent rate of H^+ entry was considerably slowed down (by nearly 40 %) and the gradient was established at a lower level (Figure 5C). These results can best be explained as the overall effect between H^+ entry facilitated by Mg^{2+}-ATPase and H^+ extrusion driven by Ca^{2+}-ATPase.

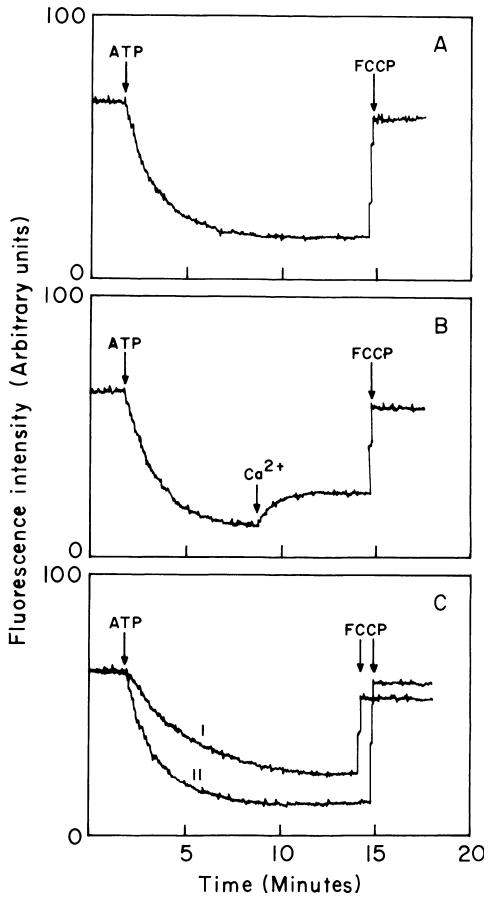

Figure 5 Ca^{2+} entry is accompanied by H^+ extrusion

BCECF-loaded vesicles (500 μl; approx. 250 μg of protein) were placed in a 1 ml cuvette and fluorescence intensity was measured as described in the Materials and methods section. (**A**) ATP (3 mM), FCCP (10 μM); (**B**) ATP (3 mM), $CaCl_2$ (100 μM), FCCP (10 μM); (**C**) in curve II, ↓ indicates addition of ATP (3 mM) and in curve I simultaneous addition of ATP (3 mM) and $CaCl_2$ (100 μM). FCCP (10 μM) additions are indicated.

DISCUSSION

The development of a method that allows preparation of sealed surface membrane vesicles of defined polarity greatly facilitates studies designed to elucidate the functional features of the plasma membrane of a particular organism or cell type. Taking advantage of the subpellicular structure of *L. donovani*, we have been able to standardize a procedure for producing sealed everted vesicles (Figure 1, bottom), which can be utilized to study ion or metabolite transport. The unsealed vesicles of original polarity (Figure 1, top) can also be sealed under appropriate conditions to supplement studies with everted vesicles (D. Mandal, T. Mukherjee, S. Sarkar, S. Majumdar and A. Bhaduri, unpublished work). These vesicles of defined polarity will be invaluable tools in elucidating ion movements, metabolite transport, drug accumulation and efflux in the parasite. Sealed vesicles were prepared from other trypanosoma [32,33] including *L. donovani* [31], but, in the absence of associated microtubular structures, their polarities could not be ascertained. Using these vesicles of undefined polarity and by measuring medium Ca^{2+} by the arsenazo method, ATP-dependent Ca^{2+} entry was demonstrated in *Trypanosoma cruzi* [32] and *Trypanosoma brucei* [33]. The internal concentration of accumulated Ca^{2+} and counter movement of H^+ were not demonstrated in these cases.

Biochemical and cytochemical studies had previously shown that both the surface membrane Ca^{2+}-ATPase and the Mg^{2+}-ATPase of this parasite are transmembrane proteins with their catalytic site facing the cytosol [17,31]. Consistent with this picture, we could show movement of Ca^{2+} (Figure 2) and H^+ (Figure 5A) into the everted vesicles on addition of ATP under appropriate conditions. At the steady-state level, the average accumulation of Ca^{2+} was 1.1 mM (Figure 2) showing the capability of plasma-membrane Ca^{2+}-ATPase to act as an extrusion pump for Ca^{2+} against a concentration gradient. The excellent correspondence between Ca^{2+}-ATPase activity and Ca^{2+} entry at all stages of enzyme inactivation and reactivation (Figure 4) leaves little doubt that this enzyme is solely responsible for the ATP-dependent Ca^{2+} movement across the plasma membrane. Further, as in the case of erythrocyte plasma-membrane Ca^{2+}-ATPase [8], the parasite enzyme also appears to be a Ca^{2+}/H^+ exchanger (Figure 5), although the exact stoichiometry could not be investigated because of the presence of the H^+-translocating Mg^{2+}-ATPase. Incorporation of purified Ca^{2+}-ATPase into liposomes alone can provide a satisfactory answer to this question and also to questions related to the various stoichiometries of Ca^{2+} entry. We are at present directing our efforts in this direction. The present work, coupled with earlier studies [11,15,16,18], leaves little doubt that a mechanism for Ca^{2+} homoeostasis exists in this human pathogen with a complex life cycle. Much work, however, needs to be carried out before the specific biomodulatory role of Ca^{2+} can be elucidated.

We thank Mr. Sailen Dey for assistance with electron microscopic photography, and also Mr. S. K. Sahu and Mr. H. N. Dutta of the Art section.

REFERENCES

1 Berridge, M. T. (1993) Nature (London) **361**, 315–325
2 Carafoli, E. (1987) Annu. Rev. Biochem. **56**, 159–193
3 Henzi, V. and Medermott, A. B. (1992) Neuroscience **46**, 251–273
4 Carafoli, E. (1988) Methods Enzymol. **157**, 3–11
5 Tanford, C., Reynold, J. A. and Johnson, E. A. (1987) Proc. Natl. Acad. Sci. U.S.A. **84**, 7094–7098
6 Carafoli, E. (1992) J. Biol. Chem. **267**, 2115–2118
7 Clarke, D. M., Loo, T. W., Inesi, G. and Maclennan, D. H. (1989) Nature (London) **239**, 476–478
8 Hao, L., Rigand, J. L. and Inesi, G. (1994) J. Biol. Chem. **269**, 14268–14275
9 Ashford, R. W., Desjeux, P. and Ruadt, P. (1992) Parasitol. Today **8**, 104–105
10 Chang, K. P., Fong, D. and Bray, R. S. (1985) in Leishmaniasis (Chang, K. P. and Bray, R. S., eds.), pp. 1–30, Elsevier, Amsterdam
11 Philosoph, H. and Zilberstein, D. (1989) J. Biol. Chem. **264**, 10420–10424
12 Ruben, L., Hutchinson, A. and Moehlman, J. (1991) J. Biol. Chem. **266**, 24351–24358
13 Vercesi, A. E., Bernardes, C. F., Hoffmann, M. E., Gadelha, F. R. and Docampo, R. (1991) J. Biol. Chem. **266**, 14431–14434
14 Moreno, S. N. J., Docampo, R. and Vercesi, A. E. (1992) J. Biol. Chem. **267**, 6020–6026
15 Vercesi, A. E., Moreno, S. N. J. and Docampo, R. (1994) Biochem. J. **304**, 227–233
16 Sarkar, D. and Bhaduri, A. (1995) FEBS Lett. **375**, 83–86
17 Ghosh, J., Ray, M., Sarkar, S. and Bhaduri, A. (1990) J. Biol. Chem. **265**, 11345–11351
18 Majumdar, S., Mukherjee, T., Ray, M. and Bhaduri, A. (1992) J. Biol. Chem. **267**, 18440–18446
19 Mukherjee, T., Mandal, D. and Bhaduri, A. (1994) Int. Congr. Biochem. Mol. Biol. India 16th Abstr. **2**, 392
20 Saha, A. K., Mukherjee, T. and Bhaduri, A. (1986) Mol. Biochem. Parasitol. **19**, 195–200.
21 Mukherjee, T., Ray, M. and Bhaduri, A. (1988) J. Biol. Chem. **263**, 708–713
22 Hatefi, Y. (1978) Methods Enzymol. **53**, 27–35
23 Sillen, L. G. and Martell, A. E. (1971) Stability Constants of Metal Ion Complexes, Special Publications 17 and 25, Chemical Society, London
24 Markwell, M. A. K., Hass, S. M., Bieber, L. L. and Tolbert, N. E. (1978) Anal. Biochem. **87**, 206–210
25 Rottenberg, H. (1979) Methods Enzymol. **55**, 547–569

26 Ruben, L., Hutchinson, A. and Mochlman, J. (1991) J. Biol. Chem. **266**, 24351–24358
27 Vickerman, K. and Pneston, T. M. (1900) in Biology of the Kinetoplastida, (Lumsden, E., eds.), pp. 35–130, Academic Press, New York
28 Dwyer, D. M. (1980) J. Protozool. **27**, 176–182
29 Dwyer, D. M. and Gottlieb, M. (1984) Mol. Biochem. Parasitol. **10**, 139–150
30 Tsao, Y. and Huang, L. (1985) Biochemistry **24**, 1092–1098
31 Zilberstein, D. and Dwyer, D. M. (1988) Biochem. J. **256**, 13–21
32 Benaim, G., Losada, S., Gadelha, F. R. and Docampo, R. (1991) Biochem. J. **280**, 715–720
33 Benaim, G., Lopez-Estrano, C., Docampo, R. and Moreno, S. N. J. (1993) Biochem. J. **296**, 759–763

Received 26 June 1996/2 October 1996; accepted 9 October 1996